Improved Modified OSAP Controller for Voltage Source PWM Inverters

Cassiano Rech, Humberto Pinheiro, Hélio L. Hey, Hilton A. Gründling and José R. Pinheiro
Power Electronics and Control Research Group – GEPOC
Federal University of Santa Maria – UFSM
97105-900 – Santa Maria, RS – Brazil
cassiano@ieee.org, renes@ctlab.ufsm.br - http://www.ufsm.br/gepoc

***Abstract* – This paper proposes an improved modified One Sampling Ahead Preview controller with repetitive control action for voltage source PWM inverters. The proposed method employs a switching frequency greater than the sampling frequency, therefore it is possible to implement this technique on a low cost microcontroller while keeping the advantages of switching at high frequency. This PWM pattern minimizes the effects of the plant modeling errors resulting from the simplifications made to obtain the linear discrete-time plant model. In addition, due to repetitive control action, this digital control scheme can minimize the steady-state error and periodic distortions caused by nonlinear cyclic loads. Plant model and theoretical analysis of the control scheme are discussed. Simulation and experimental results are presented to verify the performance of the proposed approach under different load conditions.**

I. INTRODUCTION

In recent years, digital feedback control has been widely applied to voltage source PWM (pulsewidth modulated) inverters. Among these control techniques, the microprocessor-based deadbeat control scheme is distinguished by fast response [1], [2]. The PWM signal is determined at every sampling instant by the microprocessor, based on output measurements and the reference signal. This approach can result in a low THD (total harmonic distortion) sinusoidal output with fast transient response. However, the detection of both output voltage and output capacitor current is required at each sampling instant. Thus, a deadbeat control algorithm using only a voltage sensor was proposed for PWM inverters, which may be called one sampling ahead preview (OSAP) controller [3]. In addition, a repetitive controller [4] was added to OSAP controller to minimize the steady-state error and periodic distortions caused by nonlinear cyclic loads such as rectifiers loads [5], [6]. Nevertheless, these digital control schemes have the disadvantage that the maximum available pulsewidth is limited by the acquisition and computation time of the microprocessor.

To solve this problem, modified PWM patterns [2], [7] and predictive algorithms [8] have been developed. In [8], a modified OSAP controller was proposed to increase the maximum available pulsewidth. In this approach, the pulsewidth in the *k*-th sampling interval is computed by using the output voltage sampled at the previous sampling instants. Hence, the pulsewidth is determined during the previous interval in order to extend the pulsewidth to the entire sampling interval *T*. However, this digital control technique is very sensitive to parameter variations and plant modeling errors.

This paper proposes an improved modified OSAP controller for voltage source PWM inverters, which minimizes the effects of the plant modeling errors resulting from the simplifications made to obtain a linear discrete-time plant model. This digital control scheme employs a switching frequency greater than the sampling frequency, minimizing the undesirable effects of the plant modeling errors. In addition, as the sampling frequency is smaller than the switching frequency, it is possible to implement this controller on a low speed microcontroller. In addition, a repetitive action is included to the proposed modified OSAP controller to minimize periodic errors caused by nonlinear cyclic loads.

In Section II the plant model of the proposed system is presented. The modified OSAP controller with repetitive control action is described in Section III. Section IV presents simulation results with linear and nonlinear loads. Section V shows experimental results obtained for linear and nonlinear loads based on a microcontroller-controlled system.

II. PLANT MODEL

A typical single-phase PWM inverter is shown in Fig. 1, where the full-bridge inverter, LC filter, and resistive load *R* are considered as the plant to be controlled. A triac connected in series with a resistive load or a full-bridge rectifier with capacitive filter and resistive load will be used to evaluate the performance of the system with nonlinear loads. The power circuit shown in Fig. 1 is modeled as a second-order system with the state vector $[v_c(t) \quad \dot{v}_c(t)]^T$, where $v_c(t)$ is the output voltage and $\dot{v}_c(t)$ is the derivative of $v_c(t)$. As a result, the state equation and the output equation are:

$$\begin{aligned} \dot{\mathbf{x}}(t) &= \mathbf{A}\mathbf{x}(t) + \mathbf{B}v_{in}(t) \\ y(t) &= \mathbf{C}\mathbf{x}(t) \end{aligned} \tag{1}$$

where

$$\mathbf{x}(t) = \begin{bmatrix} v_c(t) \\ \dot{v}_c(t) \end{bmatrix}, \ \mathbf{A} = \begin{bmatrix} 0 & 1 \\ -\omega_p^2 & -2\zeta_p\omega_p \end{bmatrix}, \ \mathbf{B} = \begin{bmatrix} 0 \\ \omega_p^2 \end{bmatrix},$$
$$\mathbf{C} = [1 \quad 0], \ \omega_p = \frac{1}{\sqrt{LC}}, \ \zeta_p = \frac{1}{2R}\sqrt{\frac{L}{C}} \tag{2}$$

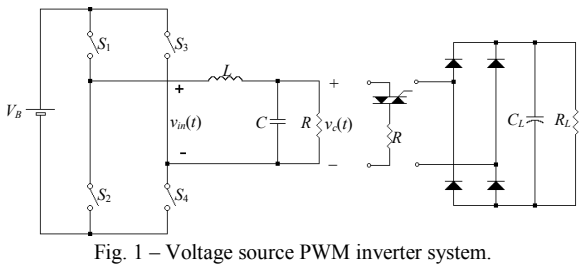

Fig. 1 – Voltage source PWM inverter system.

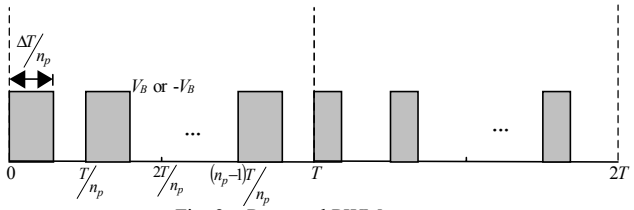

Fig. 2 – Proposed PWM pattern.

Fig. 2 shows the proposed PWM pattern. As seen in Fig. 2, the switching devices are turned on and off n_p times during each sampling interval T so that the inverter voltage $v_{in}(t)$ becomes n_p pulses of magnitude $+V_B$, $-V_B$, or zero, and width $\Delta T/n_p$. As a result, the sampled-data equation of the system at time $t=(k+1)T$ is:

$$\mathbf{x}(k+1)=e^{\mathbf{A}T}\mathbf{x}(k)+\int_0^{\frac{\Delta T(k)}{n_p}} e^{\mathbf{A}(T-\tau)}\mathbf{B}V_B\,d\tau+ \\ +\int_{\frac{T}{n_p}}^{\frac{T+\Delta T(k)}{n_p}} e^{\mathbf{A}(T-\tau)}\mathbf{B}V_B\,d\tau+....+\int_{\frac{(n_p-1)T}{n_p}}^{\frac{(n_p-1)T+\Delta T(k)}{n_p}} e^{\mathbf{A}(T-\tau)}\mathbf{B}V_B\,d\tau \tag{3}$$

Moreover, term $e^{A\Delta T/n_p}$ can be computed by using an infinite series (Taylor series), and as ΔT is smaller in magnitude than T terms of higher than ΔT^2 can be neglected [2]. Thus, from (3), the sampled-data state representation of the plant can be found as:

$$\mathbf{x}(k+1)=\begin{bmatrix} g_{11} & g_{12} \\ g_{21} & g_{22} \end{bmatrix}\mathbf{x}(k)+\begin{bmatrix} h_1 \\ h_2 \end{bmatrix}\Delta T(k) \\ y(k)=\begin{bmatrix}1 & 0\end{bmatrix}\mathbf{x}(k) \tag{4}$$

where

g_{ij} is the corresponding element of $\mathbf{G}=e^{\mathbf{A}T}$,

h_i is the corresponding element of $\mathbf{H}=\frac{1}{n_p}\left(\sum_{i=1}^{n_p} e^{i\mathbf{A}T/n_p}\right)\mathbf{B}V_B$.

The input-output representation of (4) in the Z-domain is

$$y(z)=\frac{h_1+(h_2g_{12}-h_1g_{22})z^{-1}}{z-(g_{11}+g_{22})+(g_{11}g_{22}-g_{12}g_{21})z^{-1}}\Delta T(z) \tag{5}$$

Thus, the following difference equation can be obtained:

$$y(k+1)+a_1y(k)+a_2y(k-1)=b_1u(k)+b_2u(k-1) \tag{6}$$

where the input variable and parameters are

$$u(k)=\frac{\Delta T(k)}{T}V_B \qquad b_1=h_1\,T/V_B \\ a_1=-(g_{11}+g_{22}) \qquad b_2=(h_2g_{12}-h_1g_{22})T/V_B \\ a_2=g_{11}g_{22}-g_{12}g_{21} \tag{7}$$

III. Modified OSAP Controller with Repetitive Control Action

A. Control Law

From (6), the equation of the OSAP controller [3] is obtained:

$$u_{OSAP}(k)=\frac{r(k+1)+p_1y(k)+p_2y(k-1)-q_2u(k-1)}{q_1} \tag{8}$$

where $r(k+1)$ is the reference signal at the next sampling instant, $y(k)$ and $y(k-1)$ are the output voltage at the present and the previous sampling instant, and $u(k-1)$ is the value of the control law at the previous sampling instant. If the OSAP controller gains p_1, p_2, q_1 and q_2 are equal to the plant parameters a_1, a_2, b_1 and b_2, respectively, it becomes a deadbeat control law which forces the output voltage to be equal to the reference signal at the next sampling interval. However, if the plant parameters change after the controller gains in (8) have been determined, then the deadbeat response is no longer obtained [3].

Moreover, the pulsewidth determination for k-th sampling interval is started at $t = kT$ with the sampling of the output voltage and then after the computation time the pulsewidth is determined. Consequently, the delay time caused by the output voltage A/D conversion and control law computation reduces the maximum available pulsewidth. To solve this problem, Nishida e Haneyoshi presented the modified OSAP controller [8].

By using (6) to obtain $y(k)$, and substituting in (8), then the modified OSAP controller equation [8] becomes:

$$u_{MOD}(k)=\frac{r(k+1)+P_1y(k-1)+P_2y(k-2)-Q_2u(k-1)-Q_3u(k-2)}{Q_1} \tag{9}$$

where P_1, P_2, Q_1, Q_2 and Q_3 are the controller gains, given by:

$$P_1=p_2-a_1p_1 \\ P_2=-p_1a_2 \\ Q_1=q_1 \\ Q_2=q_2-p_1b_1 \\ Q_3=-p_1b_2 \tag{10}$$

or

$$P_1=-\left(g_{11}^2+g_{11}g_{22}+g_{12}g_{21}+g_{22}^2\right) \\ P_2=-\left(g_{11}g_{12}g_{21}-g_{11}^2g_{22}+g_{12}g_{21}g_{22}-g_{11}g_{22}^2\right) \\ Q_1=h_1T/V_B \\ Q_2=(h_1g_{11}+h_2g_{12})T/V_B \\ Q_3=\left(-h_1\left(g_{11}g_{22}+g_{22}^2\right)+h_2\left(g_{11}g_{12}+g_{12}g_{22}\right)\right)T/V_B \tag{11}$$

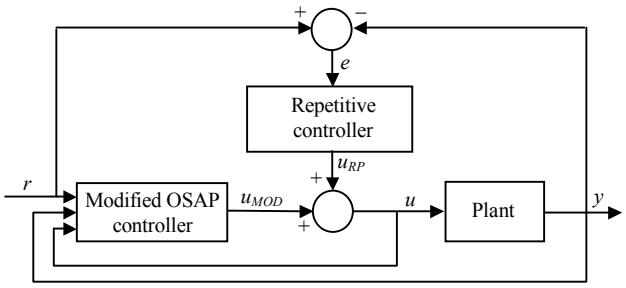

Fig. 3 – Block diagram of the control system, using the modified OSAP controller with repetitive control action.

Equation (9) shows that the required signals for the determination of the control law $u_{MOD}(k)$ are the output voltage at the previous sampling instants ($y(k-1)$ and $y(k-2)$), the values of the control law at the previous sampling instants ($u(k-1)$ and $u(k-2)$), and the reference signal at the next sampling instant ($r(k+1)$). Hence the pulsewidth determination can be completed during the previous interval, and the pulsewidth can be extended to the theoretically maximum limit, that is, the sampling interval T.

In addition, a repetitive controller is added to modified OSAP controller, as shown in Fig. 3, to minimize the steady-state error and distortions caused by periodic disturbances, such as nonlinear loads.

In a similar way to that presented in [5], the repetitive control law can be written as:

$$u_{RP}(k)=c_1 e(k+N-n)+c_2\sum_{i=1}^{\infty} e(k+N-i.n) \qquad (12)$$

where $e(k)$ is the tracking error, c_1 and c_2 are the gains of the repetitive controller, N is the time advance step size and n is the number of samples in a period of reference voltage. The repetitive controller gains are designed to guarantee a good steady-state response for any resistive load and fast convergence of the output error for nonlinear cyclic loads.

Then, the control law $u(k)$ becomes:

$$u(k)=u_{MOD}(k)+u_{RP}(k) \qquad (13)$$

B. Stability Analysis

Taking the Z-transformation of (6) and (9) and eliminating $u_{MOD}(z)$ results:

$$y(z)=\frac{(b_1 z+b_2)z^3 r(z)}{(z^2+a_1 z+a_2)(Q_1 z^2+Q_2 z+Q_3)-(P_1 z+P_2)(b_1 z+b_2)}$$

$$y(z)=G_{MOD}(z)r(z) \qquad (14)$$

where

$$G_{MOD}(z)=\frac{(b_1 z+b_2)z^3}{(z^2+a_1 z+a_2)(Q_1 z^2+Q_2 z+Q_3)-(P_1 z+P_2)(b_1 z+b_2)} \qquad (15)$$

If the modified OSAP controller gains P_1, P_2, Q_1, Q_2 and Q_3 are computed from (11), using the real plant parameters, then (15) has three poles at zero, and one pole at the plant zero ($-b_2/b_1$). Thus, (14) becomes

$$y(z)=r(z) \qquad (16)$$

This equation means that a deadbeat response is obtained with the control law (9) using exactly tuned controller gains.

However, in a similar way to OSAP controller, if the plant parameters change after the controller gains in (9) are determined for the previous plant constants, then the poles in (15) shift from the desired values and deadbeat response is no longer obtained. The trajectories of poles of (15) are shown in Fig. 4, when the load R changes its magnitude (maintaining the other parameters constants). Since the pole zero cancellation is not achieved, and also the poles move from the origin, the deadbeat response is not achieved. However, all poles are within a unit circle, so that stable operation is expected.

With the inclusion of the repetitive control, the transfer function $E(z)/R(z)$ of the system shown in Fig. 3, after Z-transformation of (6), (9), (12)–(13), is given by

$$\frac{E(z)}{R(z)}=\frac{(1-G_{MOD}(z))(1-z^{-n})}{1-z^{-n}H_{MOD}(z)} \qquad (17)$$

where the Z-transform of the output error is $E(z)$, $R(z)$ is the transformed reference input, and

$$H_{MOD}(z)=1-Q_1 z^{N-1}(c_1+c_2-c_1 z^{-n})G_{MOD}(z) \qquad (18)$$

Assuming that (14) is stable, then the stability of the system is determined by the repetitive control. From (17), it is possible to demonstrate that a sufficient condition [5] for the stability is

$$|H_{MOD}(j\omega)|\leq 1 \qquad (19)$$

where $\omega=2\pi m f$ ($m = 0, 1, 2, \ldots, n/2$).

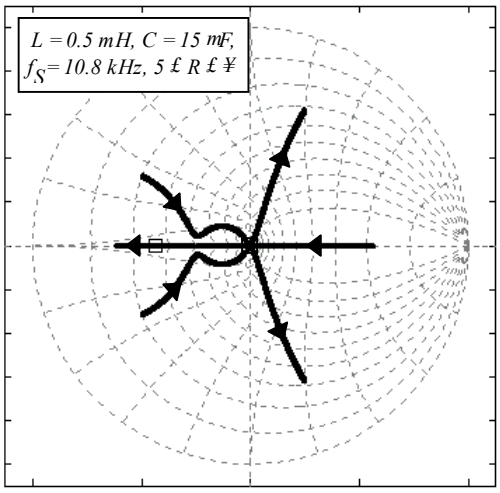

Fig. 4 – Trajectories of poles of (15) with R change in z domain.

IV. SIMULATION RESULTS

Table I gives the parameters of the single-phase PWM inverter system used in digital computer simulation (with MATLAB®) to verify the performance of the improved modified OSAP controller with repetitive control action.

TABLE I - PARAMETERS OF PWM INVERTER.

Filter inductance	L = 1 mH (Switching frequency = 10.8 kHz) L = 0.5 mH (Switching frequency = 32.4 kHz)
Filter capacitance	C = 25 µF (Switching frequency = 10.8 kHz) C = 15 µF (Switching frequency = 32.4 kHz)
DC input voltage	V_B = 100 V
Reference voltage	r = 55 V_{RMS}, f = 60 Hz
Nominal resistive load	R = 12 Ω
Nonlinear load	R_L = 25 Ω C_L = 330 µF
Sampling frequency	f_S = 10.8 kHz
Sampling period	T = 92.6 µs

Initially, the modified OSAP controller with repetitive control action ($c_1 = 0.1$ and $c_2 = 0.3$) was simulated using a PWM pattern with one pulse centered in the sampling interval. Fig. 5(a) shows the output voltage $v_c(t)$ and load current $i_L(t)$ waveforms for nominal resistive load (12 Ω) and Fig. 5(b) presents the output voltage $v_c(t)$ and load current $i_L(t)$ waveforms for no-load. Fig. 6 shows the response of the modified OSAP controller for nominal resistive load, using a PWM pattern with one pulse in the beginning of the sampling interval.

Due to simplifications realized to obtain the linear discrete-time model, it can be observed that the modified OSAP controller does not present a good performance using these PWM patterns.

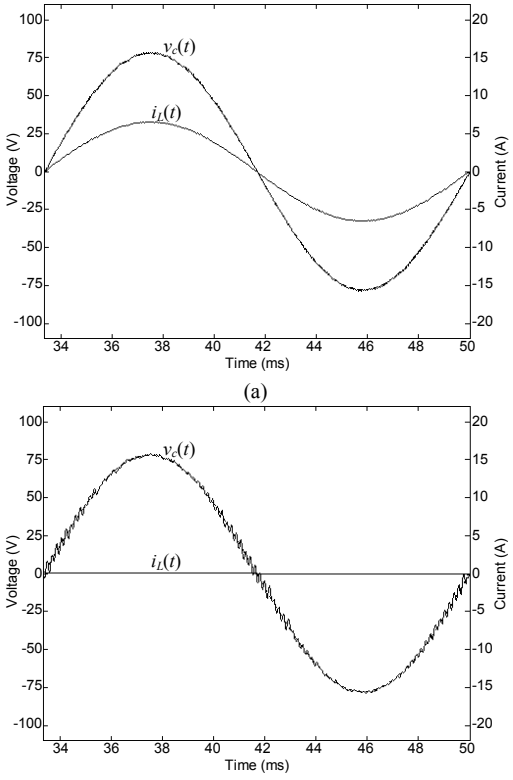

Fig. 5 – Response of the modified OSAP controller with repetitive control action for a PWM pattern with one pulse centered in sampling interval. (a) Nominal resistive load. (b) No-load.

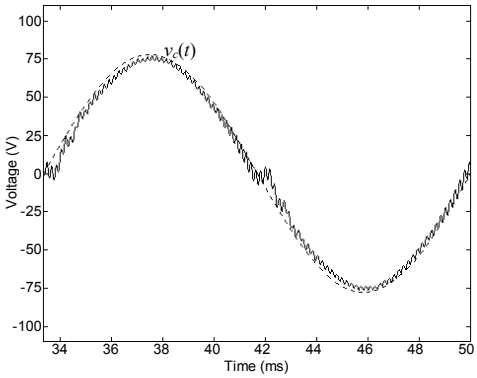

Fig. 6 – Response of the modified OSAP controller for nominal resistive load, using a PWM pattern with one pulse in the beginning of the sampling interval.

However, it was verified that the plant modeling errors resulting from the simplifications made to obtain the discrete-time plant model are smaller when the output filter parameters are decreased, maintaining the same sampling frequency. Then, to minimize the effects of the plant modeling errors, the switching frequency was increased and, consequently, the output filter parameters were reduced, as shown in Table I. Then, this controller has been simulated using a PWM pattern with three voltage pulses in a sampling frequency. With this, the pulsewidth is updated at each three switching periods. Fig. 7(a) presents the response of the modified OSAP controller with repetitive control action, using the proposed PWM pattern, for nominal resistive load. Fig. 7(b) shows the output voltage and load current waveforms for no-load.

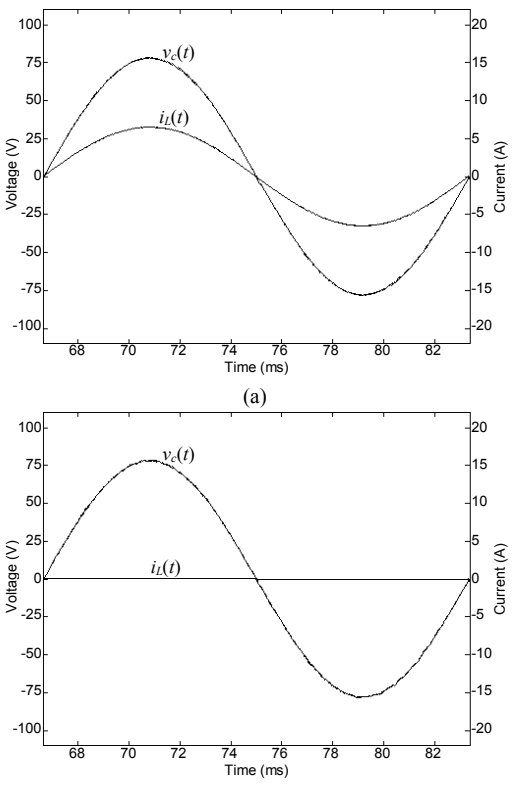

Fig. 7 – Output voltage $v_c(t)$ and load current $i_L(t)$ waveforms for linear loads, by using the proposed PWM pattern. (a) Nominal resistive load. (b) No-load.

Fig. 8(a) shows the response of the improved modified OSAP controller for nominal resistive load in series with a triac commuting at 72º/252º. Fig. 8(b) presents the response of the improved modified OSAP controller, with the inclusion of the repetitive controller, for the same nonlinear cyclic load. It can be observed that the periodic errors caused by this nonlinear cyclic load are reduced with the inclusion of the repetitive controller.

Fig. 9 presents the output voltage $v_c(t)$ and load current $i_L(t)$ waveforms for the same nonlinear cyclic load including an unmodeled zero at –80000 rad/s. This unmodeled stable zero could be physically represented by an unmodeled equivalent series resistance (ESR) of 0.5 Ω of the filter capacitor. It is observed that the proposed controller presents a good performance even in the presence of this unmodeled dynamic.

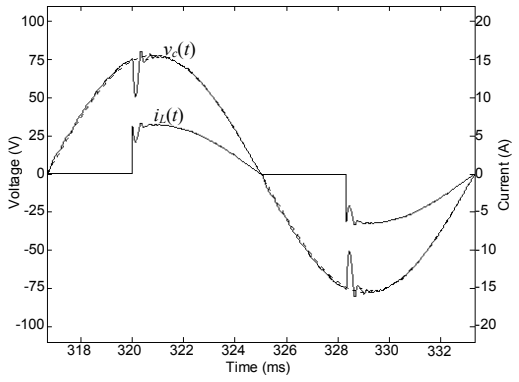

(a)

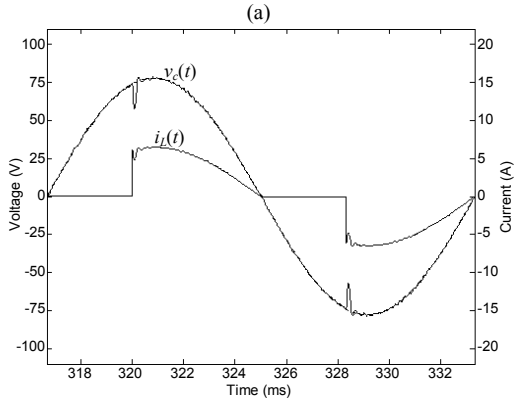

(b)

Fig. 8 – Output voltage $v_c(t)$ and load current $i_L(t)$ waveforms for nominal resistive load in series with a triac commuting at 72º/252º. (a) Without repetitive controller. (b) With repetitive controller.

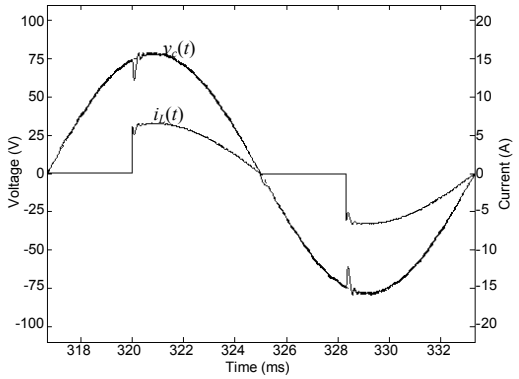

Fig. 9 – Output voltage $v_c(t)$ and load current $i_L(t)$ waveforms for nominal resistive load in series with a triac commuting at 72º/252º with the inclusion of an unmodeled stable zero at -80000 rad/s.

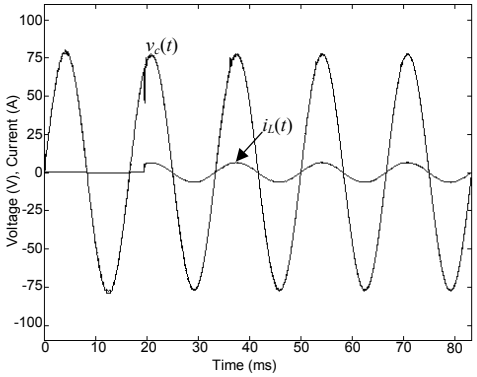

Fig. 10 – Output voltage $v_c(t)$ and load current $i_L(t)$ waveforms under a step load change from no-load to full-load.

In Fig. 10 are shown the output voltage $v_c(t)$ and load current $i_L(t)$ waveforms under a step load change from no-load to full-load, demonstrating the good transient response of the proposed controller for a step load change.

V. Experimental Results

A laboratory prototype of the single-phase PWM inverter using IGBT's has been built to verify the performance of the improved modified OSAP controller with repetitive control action. The component values of the inverter system are the same used in simulation (Table I). It is important consider that the real plant includes some unmodeled dynamics (ESR's, dead time, etc.) that can affect the performance of the controller. In this way, the plant modeling must be made carefully to obtain a good performance.

The simplified block diagram of the experimental setup is shown in Fig. 11. The controller has been implemented using an 8-bit data word microcontroller (PIC17C756 of Microchip Technology Inc.). It has an embedded 10 bits A/D converter and a PWM signal generator that reduce the PWM inverter control circuitry. The computation time (output voltage A/D conversion time and control law computation) spent by the PIC17C756 does not allow to increase the sampling frequency, however the PWM signal frequency can be equal to 32.4 kHz with an 8-bit resolution. The PWM signal frequency could be increased, but its resolution would decrease and the controller performance would be affected.

Fig. 12 shows the response of the modified OSAP controller for nominal load, using a PWM pattern with one voltage pulse in the beginning of the sampling interval (sampling frequency equal to switching frequency).

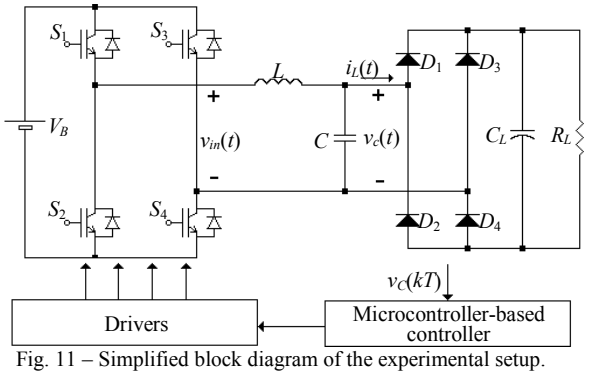

Fig. 11 – Simplified block diagram of the experimental setup.

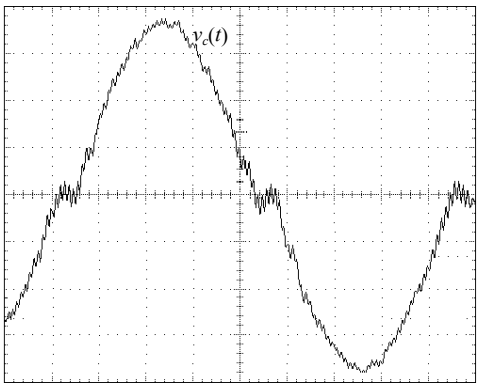

Fig. 12 – Output voltage $v_c(t)$ (20V/div) waveform for nominal resistive load, using the PWM pattern with one pulse in the beginning of the sampling interval. Time scale: 2 ms/div.

It can be observed in Fig. 12 that the modified OSAP controller really does not present a good performance using this PWM pattern.

On the other hand, Fig. 13 shows the output voltage $v_c(t)$ (THD = 1.52%) and load current $i_L(t)$ waveforms for nominal resistive load, using the improved modified OSAP controller with repetitive control action. Fig. 14 presents the output voltage $v_c(t)$ (THD = 1.36%) and load current $i_L(t)$ waveforms for no-load.

To check the response of the proposed control scheme for nonlinear loads, the resistive load was replaced by a single-phase rectifier with capacitive filter and resistive load, as shown in Fig. 11. Fig. 15 shows the output voltage $v_c(t)$ (THD = 2.34%) and load current $i_L(t)$ waveforms for a rectifier-RC load.

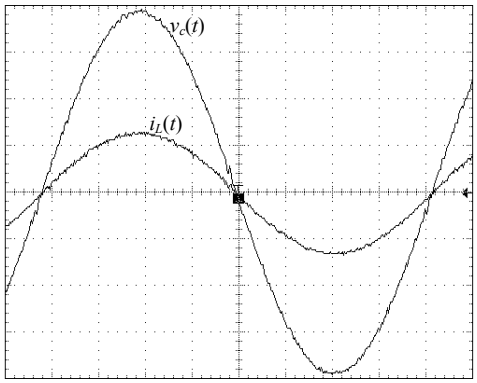

Fig. 13 – Output voltage $v_c(t)$ (20V/div) and load current $i_L(t)$ (5A/div) for nominal resistive load, using the proposed PWM pattern. Time scale: 2 ms/div.

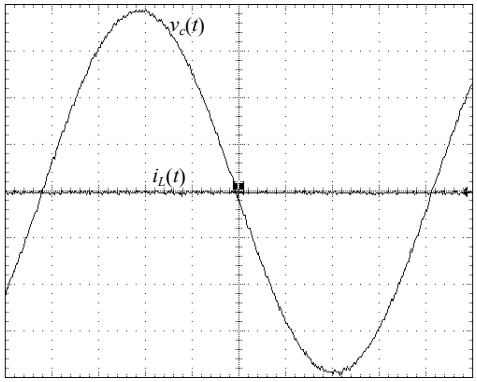

Fig. 14 – Output voltage $v_c(t)$ (20V/div) and load current $i_L(t)$ (5A/div) for no-load, using the proposed PWM pattern. Time scale: 2 ms/div.

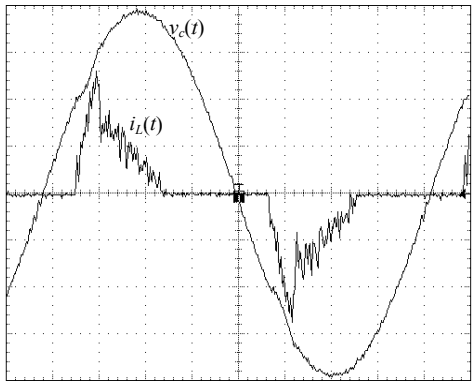

Fig. 15 – Output voltage $v_c(t)$ (20V/div) and load current $i_L(t)$ (5A/div) for rectifier-RC load, using the proposed PWM pattern. Time scale: 2 ms/div.

VI. CONCLUSIONS

This paper presents an improved modified OSAP controller with repetitive control action for single-phase PWM inverters. Results show that the proposed control scheme can minimize periodic distortions caused by nonlinear cyclic loads. Moreover, the increase of the switching frequency minimizes the effects of the plant modeling errors resulting from the simplifications made to obtain a linear discrete-time plant model. With the increasing of the switching frequency, the output filter parameters can be reduced, decreasing the weight and the volume of the system. In addition, as the sampling frequency is smaller than the switching frequency, it is possible to implement this controller on a low speed microcontroller. Stability analysis accomplished in this paper demonstrates that the closed-loop system is stable for any resistive load. Experimental results shows that even with the limitations of the processing speed and fixed-point routines, this control algorithm performs well.

REFERENCES

[1] K. P. Gokhale, A. Kawamura and R. G. Hoft, "Dead beat microprocessor control of PWM inverter for sinusoidal output waveform synthesis", *IEEE Trans. on Ind. Applications*, v. IA-23, n. 5, pp. 901-910, Sept./Out. 1987.

[2] A. Kawamura, R. Chuarayapratip and T. Haneyoshi, "Deadbeat control of PWM inverter with modified pulse patterns for uninterruptible power supply", *IEEE Trans. on Ind. Electronics*, v. 35, n. 2, pp. 295-301, May 1988.

[3] A. Kawamura, T. Haneyoshi and R. G. Hoft, "Deadbeat controlled PWM inverter with parameter estimation using only voltage sensor", *IEEE Trans. on Power Electronics*, v. 3, n. 2, pp. 118-125, Apr. 1988.

[4] S. Hara, Y. Yamamoto, T. Omata and M. Nakano, "Repetitive control system: A new type servo system for periodic exogenous signals", *IEEE Trans. on Automatic Control*, v. 33, n. 7, pp. 659-667, Jul. 1988.

[5] T. Haneyoshi, A. Kawamura and R. G. Hoft, "Waveform compensation of PWM inverter with cyclic fluctuating loads", *IEEE Trans. on Industry Applications*, v. 24, n. 4, pp. 582-588, Jul./Aug. 1988.

[6] K. Zhou and D. Wang, "Repetitive controlled 3-phase CVCF PWM inverter", in *IEEE Industrial Electronics Conference* , pp. 480-484, 1999.

[7] C. Hua, "Two-level switching pattern deadbeat DSP controlled PWM inverter", *IEEE Trans. on Power Electronics*, v. 10, n. 3, pp. 310-317, May 1995.

[8] Y. Nishida and T. Haneyoshi, "Predictive instantaneous value controlled PWM inverter for UPS", in *IEEE Power Electronics Specialists Conference*, v. 2, pp. 776-783, 1992.